

Phase transition between the cholesteric and twist grain boundary C phases

I. Luk'yanchuk^{1,2,*}

¹*L.D.Landau Institute for Theoretical Physics, Moscow, Russia.*

²*Departamento de Fisica, Universidade Federal de Minas Gerais, Caixa Postal 702, 30161-970, Belo Horizonte, Minas Gerais, Brazil*

(October 11, 2018)

Abstract

The upper critical temperature T_{c2} for the phase transition between the Cholesteric phase (N^*) and the Twist Grain Boundary C phase with the layer inclination tilted to the pitch axis (TGB_{Ct}) in thermotropic liquid crystals is determined by the mean field Chen-Lubensky approach. We show that the N^* - TGB_{Ct} phase transition is split in two with the appearance of either the TGB_A or the TGB_{2q} phase in a narrow temperature interval below T_{c2} . The latter phase is novel in being superposed from two degenerate TGB_{Ct} phases with different (left and right) layers inclinations to the pitch axis.

Typeset using REVTeX

I. INTRODUCTION

A Twist Grain Boundary (*TGB*) state that appears as an intermediate state at the Cholesteric (N^*) - Smectic (*Sm*) phase transition in chiral thermotropic liquid crystals was predicted theoretically by Renn and Lubensky [1] in 1988 and then, one year later, was independently observed experimentally [2,3]. Since that time a wealth of properties of this new state were discovered in a number of experimental [4–13] and theoretical [14–17] investigations.

The results of these studies and the results of the present paper are summarized in the phase diagram of Fig. 1 where the parameters t, σ_{\perp} (whose meanings will be explained in Sect. II) are controlled by the following experimental conditions: temperature, concentration, pressure etc. The reason for such a variety of intermediate phases is that, the direct N^* -*Sm* transition can not occur in a continuous way since the cholesteric twist of the director, $\mathbf{n}(r) = (0, \sin(k_0x), \cos(k_0x))$, is incompatible with the smectic layered structure. The last one in chiral liquid crystals is known to be of either *SmA* or *SmC** type: in *SmA* the director \mathbf{n} is parallel to the layers modulation vector \mathbf{q} whereas in *SmC** it is tilted with respect to \mathbf{q} by a constant angle θ_0 and forms a conical precession along the normal to layers. Therefore, the transition occurs either by the first order untwisting of $\mathbf{n}(r)$ or via formation of intermediate *TGB* phases. The actual sequence of the intermediate phases depends on the final *Sm* state that occurs at low temperature. There is only one intermediate phase (*TGB_A*) when the transition goes to *SmA* [1,14] and a series of phases when the transition goes to *SmC** [15].

The general structure of the *TGB* state is shown in Fig. 2a. The compromise between the cholesteric twist of $\mathbf{n}(r)$ and layered structure of *SmA, C** is achieved by formation of a set of rotated smectic slabs (blocks), normal to those being follow the pitch $\mathbf{n}(r)$. The slabs are separated by grain boundaries consisting of a series of equally spaced screw dislocations that provide the junction of the layers in adjoining slabs. The slab width l_b , dislocation spacing l_d , director pitch P , and layer spacing d are related by the following topological constraint [1]:

$$2\pi l_b l_d = Pd \tag{1}$$

Coupling of the director with the modulation vector \mathbf{q} results in the unbending of $\mathbf{n}(r)$ close to the block center. When temperature decreases the director pitch and slab width diverge with further untwisting of $\mathbf{n}(r)$. Finally, they tend to infinity corresponding to the transition to the *Sm* state.

The variety of *TGB* phases in Fig.1 is provided by the different internal structure of *TGB* blocks that are shown in Fig.2b-e. Generally, *TGB* blocks are reminiscent of the final *Sm* state that occurs at low temperature. Therefore, the *TGB_A* block is just the *SmA* slab, shown in Fig. 2b, confined by grain boundaries, the layers modulation vector \mathbf{q} being parallel to the director \mathbf{n} in the slab center [1]. Similarly, the *TGB_C* slab is provided by smectic layers that are inclined to \mathbf{n} by the angle $\sim \theta_0$. The inclination, however, can be done in other ways: when tilted layers are either parallel to the pith axis x as in Fig. 2b, or tilted to it as in Fig.2c. We call these phases *TGB_{C_p}* and *TGB_{C_t}*. The blocks of the *TGB_{C_p}* and *TGB_{C_t}* phases actually have the structure of slabs of differently oriented *SmC*, as distinguished from

its chiral analog SmC^* by the absence of the director precession. Under certain conditions a transition $SmC \rightarrow SmC^*$ occurs inside the TGB_C slabs [15]. The corresponding TGB_{C^*} phase that appears close to the bulk SmC^* phase (see Fig. 1) will be not considered in this paper.

Originally the TGB_{Cp} phase was assumed to be an intermediate TGB state at the N^*-SmC^* transition [15] (there it was called TGB_C). However, x-ray experiments [7] and theoretical estimations [17] demonstrate that the TGB_{Ct} phase is indeed more stable. In [17] this phase was called as the Melted Grain Boundary (MGB) phase to stress that the smectic order parameter vanishes at grain boundaries because of the small distance between screw dislocations. We prefer, however, to use the TGB_{Ct} notation to emphasize the geometrical structure of this phase.

In this paper we revise the calculation of [15] for the *upper critical temperature* T_{c2} (M_A - M_0 - M_1 - M_C line in Fig. 1 for the N^*-TGB_C transition, taking into account the recent proof of the stability of the TGB_{Ct} phase [7,17] that was not considered in [15]. We confirm and expand the estimation of [15] to the whole region of parameters. In addition we calculate the principal parameters of the TGB_{Ct} phase: upper critical temperature, slab width l_b and the X-ray diffraction pattern that can be measured experimentally.

Several features that modify the phase diagram calculated in [16,15] follow from our analysis. The TGB_A phase that was shown in [1,14] to be stable when the transition is to the SmA phase, penetrates also into the SmC^* region as a narrow stripe in between the N^* and TGB_{Ct} phases, and finishes in the tetracritical point M_0 far inside this region. The N^*-TGB_{Ct} transition is split either by this TGB_A stripe or by the narrow region of the new TGB_{2q} phase. The TGB_{2q} slab is superposed from two equivalent SmC populations with left and right layers inclined to the pitch axis as shown in Fig. 2e.

This new phase can be viewed as a kind of standing density wave quantized by the grain boundaries. In reality it can be observed in between the N^*-TGB_A - TGB_{Ct} - TGB_{2q} tetracritical point M_0 and the point M_1 . Location of these points is calculated in this paper. The upper critical temperature T_{c2} should have a kink at M_0 . Under certain conditions the enhancement (oscillation) of T_{c2} between M_0 and M_1 can be observed.

A remarkable feature of the TGB_A phase was noted in [1] to be an analogy with the Abrikosov vortex state in superconductors in a magnetic field. This completed an analogy between the superconducting transition in metals and the phase transition between Nematic (N) and SmA phases in liquid crystals, first pointed by de Gennes [18,19]. In the present article we show that the TGB_{Ct} phase is the analog of the mixed state in superconductors with a space-modulated order parameter (like Larkin-Ovchinnikov-Fulde-Ferrel phases [20,21]), providing that modulation is perpendicular to the magnetic field. Another interesting analogy we discuss is the similarity between the TGB_A - TGB_{Ct} transition and the transition between the symmetry differing phases in an "unconventional" superconductor UPt_3 in the magnetic field [22].

II. BASIC EQUATIONS

A. The chiral Chen-Lubensky Model

On a quantitative level, the appearance of *TGB* state is described by the Chen-Lubensky (CL) model [23], which is known to be a quite general approach in explaining various phase transitions between cholesteric (nematic) phases and modulated smectic phases. In this model the cholesteric and smectic phases are described by two coupled order parameters: by the twisted director $\mathbf{n}(r)$ and the space modulated complex function $\psi(r)$, where the modulation of the smectic density is given by the real part of $\psi(r)$. The resulting energy consists of two parts:

$$\mathcal{F}_{CL} = \mathcal{F}_\psi + \mathcal{F}_F \quad (2)$$

where the elastic Frank energy:

$$\begin{aligned} \mathcal{F}_F = & \frac{1}{2}K_1 (\text{div } \mathbf{n})^2 + \frac{1}{2}K_2 (\mathbf{n} \cdot \text{curl } \mathbf{n} - k_0)^2 \\ & + \frac{1}{2}K_3 (\mathbf{n} \times \text{curl } \mathbf{n})^2 \end{aligned} \quad (3)$$

provides the twisted texture of the director. In the cholesteric phase $\mathbf{n}(r) = (0, \sin(k_0x), \cos(k_0x))$. The chirality is provided by the parameter k_0 . When $k_0 = 0$, expression (3) reduces to the elastic energy of the nematic phase with $\mathbf{n} = \text{const}$.

The smectic state is described by the Ginzburg-Landau (GL) functional \mathcal{F}_ψ , which has a finite- q instability for the order parameter $\psi(r)$ provided by a gauge derivative $\mathbf{D} = \nabla - iq_0\mathbf{n}$:

$$\begin{aligned} \mathcal{F}_\psi = & a(T - T_{NA}) |\psi|^2 + \frac{1}{2}g |\psi|^4 + (C_\parallel n_i n_j \\ & + C_\perp (\delta_{ij} - n_i n_j)) (\mathbf{D}_i \psi) (\mathbf{D}_j \psi)^* + D (\mathbf{D}^2 \psi) (\mathbf{D}^2 \psi)^* \end{aligned} \quad (4)$$

We take the quartic in the gradient term in the isotropic form $D (\mathbf{D}^2 \psi) (\mathbf{D}^2 \psi)^*$ which is slightly different from the original CL model where this term was written as: $D_\perp (\delta_{ij} - n_i n_j) (\delta_{kl} - n_k n_l) (\mathbf{D}_i \mathbf{D}_j \psi) (\mathbf{D}_k \mathbf{D}_l \psi)^*$. This does not change the final results but simplifies the calculations.

Now we give a brief review of the properties of the CL model. In the nonchiral case (when $k_0 = 0$), a second order phase transition from nematic to smectic phases takes place [23]. The type of the smectic phase depends on the sign of C_\perp (terms with C_\parallel and D are assumed to be positive). When $C_\perp > 0$, a transition to the *SmA* phase with the order parameter $\psi(r) \sim \psi_0 e^{iq_0 \mathbf{n}r}$ occurs at $T = T_{NA}$. When $C_\perp < 0$ an additional transversal to \mathbf{n} modulation occurs, resulting in a *SmC* order parameter $\psi(r) \sim \psi_0 e^{i\mathbf{q}r}$ with $\mathbf{q} = (q_0 \mathbf{n}, \mathbf{q}_C)$. This modulation is stabilized by the quartic gradient term at wave vector $q_C = (-C_\perp / 2D)^{1/2}$ which gives the layers inclination angle as $\theta_0 = \arctan(q_C / q_0) = \arctan(-C_\perp / 2Dq_0^2)^{1/2}$. The *N-SmC* transition occurs at $T_{NC} = T_{NA} + C_\perp^2 / 4D$.

In a chiral case [14] (when $k_0 \neq 0$), the situation is more complicated since the gauge derivatives and anisotropic coefficients in the gradient terms in Eq.(4) depend on the direction of \mathbf{n} which is not uniform in a space. This provides a coupling of the order parameters $\mathbf{n}(r)$ and $\psi(r)$ leading to an untwisting of $\mathbf{n}(r)$ when the smectic layers are formed. Such

a process occurs either directly, by the first order transition, or via the intermediate *TGB* state. In both cases the final smectic phases are again either *SmA* or *SmC*.

The scenario of the phase transition depends on the parameters of the CL model. We formulate those conditions below. When the direct N^* -*SmA*, C^* transition takes place, the critical temperatures are calculated by comparison of the energies of the N^* and *SmA*, C^* phases [14]. The N^* -*SmA*-*SmC** tricritical point in the (T, C_\perp) plane was found to be:

$$(T^*, C_\perp^*) = (T_{NA} - (gK_2)^{1/2}k_0/a, (gK_2^3)^{1/2}k_0/2aK_3q_0^2) \quad (5)$$

The transition lines are given by:

$$\begin{aligned} T_{N^*A} &= T^*, \quad C_\perp > C_\perp^* \\ T_{AC^*} &= T_{NA} + (T_{N^*A} - T_{NA}) \cdot C_\perp^*/C_\perp, \quad C_\perp < C_\perp^* \\ T_{N^*C^*} &= T_{N^*A} + (C_\perp - C_\perp^*)^2/4aD, \quad C_\perp < C_\perp^* \end{aligned} \quad (6)$$

When the transition occurs via an intermediate *TGB* state, the critical temperatures and the detailed structure of the *TGB* state are provided by a nonuniform solution of the GL equation obtained from (4):

$$\begin{aligned} &a \left(T - T_{NA} - \frac{C_\perp^2}{4D} \right) \psi + g |\psi|^2 \psi \\ &= (C_\parallel - C_\perp) (\mathbf{nD})^2 \psi - D \left(-\mathbf{D}^2 + \frac{C_\perp}{2D} \right)^2 \psi \end{aligned} \quad (7)$$

where, $\hat{A}^2\psi = \hat{A}(\hat{A}\psi)$.

In this paper we are interested in the structure of the *TGB* state just below the N^* -*TGB* phase transition that takes place at *the upper critical temperature* T_{c2} . We consider the case when $C_\perp < 0$, that is when the system has a tendency to form the *SmC** phase at low temperature. In the following subsection we derive the basic equations that describe this transition.

B. Cholesteric-*TGB* transition

The order parameter in the *TGB* state below T_{c2} is given by a periodic superposition of rotating blocks equally shifted by a distance l_b

$$\psi(r) = \sum_m e^{i\gamma m} f(x + ml_b) e^{i\mathbf{q}_\perp m \mathbf{r}} \quad (8)$$

The component of the modulation vector transverse to the pitch $\mathbf{q}_\perp m = q_0 (0, \sin(k_0 ml_b + \varphi), \cos(k_0 ml_b + \varphi))$, follows the director twist: $\mathbf{n}(r) = (0, \sin(k_0 x), \cos(k_0 x))$ with phase advance (retardation) φ . Factors $e^{i\gamma m}$ are the degenerate phason degrees of freedom [1].

The *block profile function* $f(x)$ is localized within the block width l_b and, together with the phase φ , provides the structure of the *TGB* slab. In the *TGB*_A phase $\varphi = 0$ and $f(x)$ is a centered bell-shape function (which has a Gaussian profile $\exp(-k_0 x^2/2q_0)$ at $C_\perp \gg 0$ [1]).

The structure of the TGB_{Cp} slab (Fig. 2c) is given by a centered bell-shape function $f(\bar{x})$ and nonzero advancing (retarding) phase angle $\varphi \simeq \theta_0$ [15] that results in the tilting of the layers parallel to the pitch axis. In the TGB_{Ct} phase the angle φ is equal to zero and $f(x)$ is modulated in the x direction as $\exp(\pm i\theta x)$. This corresponds to the right (left) transverse inclination of the layers as shown in Fig. 2d.

The profile function $f(x)$ of the slab, located at the origin, and phase φ are found by solving of Eq.(7) with the substitution $\psi(r) = f(x)e^{i\mathbf{q}_\perp \cdot \mathbf{r}} \simeq f(x)e^{iq_0(z+\varphi y)}$.

Several simplifications are used in Renn-Lubensky theory. Usually the block width l_b is much smaller than the cholesteric pitch $P = 2\pi/k_0$. Therefore, on the scale of l_b the twist of $\mathbf{n}(r)$ is minimal and approximately is written as $\mathbf{n}(r) \approx (0, k_0 x, 1 - (k_0 x)^2/2)$. Next, just below T_{c2} the amplitude of $f(x)$ is small and only the terms linear in $f(x)$ are relevant in Eq.(7).

The corresponding linearized equation for $f(x)$ and φ is:

$$a(T - T_{NA} - C_\perp^2/4D)f = -\mathcal{H}f \quad \text{where} \quad (9)$$

$$\begin{aligned} \mathcal{H} = D & \left(-\partial_x^2 + (q_0 k_0)^2 (x - \varphi/k_0)^2 + \frac{C_\perp}{2D} \right)^2 \\ & + (C_\parallel - C_\perp) \frac{q_0^2 k_0^4}{4} (x^2 - 2x\varphi/k_0)^2 \end{aligned}$$

This equation has a set of localized eigenstates $f_n(x)$ with a discrete spectrum of *eigen-temperatures* T_n . The upper critical temperature T_{c2} of the N^* - TGB transition is provided by the maximal value of T_n . The block profile function is given by the corresponding eigenfunction $f_{nc2}(x)$.

We assume further that $\varphi = 0$, that is, the parallel layers' inclination according to [17] does not occur. The justification of this approximation will be presented in Sect. IIID.

It is convenient to use the dimensionless units:

$$\begin{aligned} \bar{x} = q_0 x, \quad \bar{\partial}_x = q_0^{-1} \partial_x, \quad \sigma_\parallel = \frac{C_\parallel}{4Dq_0^2}, \quad \sigma_\perp = -\frac{C_\perp}{2Dq_0^2}, \\ t = a(T - T_{NA})/Dq_0^4, \quad b = k_0/q_0, \quad \bar{\mathcal{H}} = \mathcal{H}/Dq_0^4 \end{aligned} \quad (10)$$

We discuss first the values of parameters $b, \sigma_\perp, \sigma_\parallel$. Parameter b has a sense of the power of the cholesteric twist. Usually in chiral liquid crystals the interlayer smectic spacing is much smaller than cholesteric pitch having $b \ll 1$. The small tilting angle θ_0 results in $\sigma_\perp = \tan^2 \theta_0 \ll 1$. In contrast, parameter σ_\parallel , which is related to the ratio of the layer compression elastic constant $C_\parallel q_0^2$ to the layer curvature energy Dq_0^4 , is larger than one [17,24] and therefore is much large than σ_\perp .

Neglecting C_\perp in comparison with C_\parallel in the last term of Eq.(9), we rewrite it in dimensionless units as:

$$(t - \sigma_\perp^2)f = -\bar{\mathcal{H}}f \quad \text{where} \quad (11)$$

$$\bar{\mathcal{H}} = \left(-\bar{\partial}_x^2 + b^2 \bar{x}^2 - \sigma_\perp \right)^2 + \sigma_\parallel b^4 \bar{x}^4$$

The order parameter $\psi(r)$ of the TGB state is reproduced by substitution of corresponding eigenfunction $f(x)$ into (8). Then, one can calculate the free energy \mathcal{F}_{CL} (8) of the TGB state as a function of the slab width l_b or, more conveniently, as a function of the geometrical factor l_b/l_d . The actual value of this ratio is found by minimization of \mathcal{F}_{CL} with respect to l_b/l_d . It was found [1] that $l_b/l_d \simeq 0.9\varepsilon$ when $C_\perp \gg 0$ and the TGB_A phase has a Gaussian profile in the slab. The factor ε depends the relative strengths of cholesteric splay (bend) and the twist elastic energies $K_{1,3}/K_2$. It varies from $\varepsilon = 0$ when $K_{1,3}/K_2 = 0$ (the calculation in this case is reduced to minimizing the Abrikosov factor $\beta = \langle \psi^4 \rangle / \langle \psi^2 \rangle^2$), to $\varepsilon \sim 1.5$ when $K_{1,3}/K_2$ is large. We will use this result to evaluate l_b/l_d in the $TGB_{A,Ct}$ phases when $C_\perp < 0$.

III. RESULTS

A. General

In this section we calculate the eigenstates of Eq.(11) that correspond to the upper critical temperature t_{c2} , and discuss the block structure just below t_{c2} for the different types of TGB state at $\sigma_\perp > 0$.

Note that eigentemperatures t_n (including t_{c2}) and eigenfunctions $f_n(x)$ are generally functions of $b, \sigma_\perp, \sigma_\parallel$. Because of the scaling properties resulting from Eq.(11):

$$\begin{aligned} t_n(b, \sigma_\parallel, \sigma_\perp) &= \sigma_\perp^2 \cdot t_n(b/\sigma_\perp, \sigma_\parallel, 1), \\ f_n(\bar{x}, b, \sigma_\parallel, \sigma_\perp) &= f_n(\sigma_\perp^{1/2}\bar{x}, b/\sigma_\perp, \sigma_\parallel, 1). \end{aligned} \quad (12)$$

parameter σ_\perp can be excluded if one considers the dependence $t_n(b)$ on the rescaled coordinates $b/\sigma_\perp, t/\sigma_\perp^2$.

To proceed with the diagonalization of Eq.(11) for $\sigma_\perp > 0$, recall first the results of [1,14] for the opposite case of $\sigma_\perp < 0$ when a transition occurs to the TGB_A phase. When $|\sigma_\perp|$ is large enough, the operator $\overline{\mathcal{H}}$ was shown [1] to be truncatable to the more simple form of the harmonic oscillator $-2\sigma_\perp \left(-\overline{\partial}_x^2 + b^2\overline{x}^2 \right) + \sigma_\perp^2$. The lowest eigenstate gives the Gaussian profile $e^{-b\overline{x}^2}$ of the TGB_A block and the upper critical temperature $t_{c2} = 2\sigma_\perp b$. This result can be improved if one considers the residual part of $\overline{\mathcal{H}}$ as a perturbation:

$$t_{c2} = 2\sigma_\perp b - (1 + 3\sigma_\parallel/4)b^2 \quad (13)$$

The second term is smaller than the first one if $-\sigma_\perp/b > 0.5 + 0.38\sigma_\parallel$, which is the condition of applicability of the approximation. The opposite case of $\sigma_\perp/b \sim 0$ will be discussed later.

Figure 3 shows the result of numerical diagonalization of (11) for different σ_\parallel when $\sigma_\perp > 0$. We use the $t/\sigma_\perp^2, b/\sigma_\perp$ coordinates to trace the two highest eigentemperatures (the maximal one corresponds to t_{c2}) as function of b . Note first the concurrence of two eigenstates with close eigentemperatures t_+ and t_- that give the upper critical temperature $t_{c2} = \max(t_+, t_-)$. These levels often cross when b changes, resulting in the oscillating behavior of $t_{c2}(b)$. The oscillations of $t_{c2}(b)$ are strong at $\sigma_\parallel = 0$ and more pronounced still at large values of σ_\parallel .

The appearance of these nearly degenerate eigenstates is related to two equivalent, right and left inclinations of layers in the TGB_{Ct} slab. The corresponding block profile functions,

$f_R(\bar{x})$ and $f_L(\bar{x})$, however, can not be the eigenfunctions of Eq.(11) since they do not possess the definite parity with respect to the symmetry operation $x \rightarrow -x$, which is a property of $\overline{\mathcal{H}}$. The proper eigenstates f_{\pm} with eigentemperatures t_{\pm} are constructed as superpositions of both populations as $f_{\pm} = f_R \pm f_L$ that results in the TGB_{2q} phase just below t_{c2} . The function $f_{\pm}(x)$ has cos- (sin-) like oscillations and can be viewed as a standing wave between the grain boundaries. The effects of commensurability of this wave with block width l_b stabilize either the even cos-like or the odd sin-like behavior as the lowest state to have a vanishing order parameter at the grain boundaries. The block width l_b changes as a function of b that alternates the order of the f_{\pm} eigenstates leading to the oscillations in $t_{c2}(b)$.

The tendency to SmC slab formation at lower temperatures results in the further transition from the TGB_{2q} to TGB_{Ct} phase determined by the lowest from t_+ , t_- critical temperatures renormalized by the nonlinear term $g|\psi|^2\psi$ in Eq.(7). Below this second transition, one of the populations starts to be suppressed and a block profile function is constructed now from both the f_+ and f_- eigenstates to form the TGB_{Cp} phase with either a f_L or f_R profile of the slab.

Therefore, we conclude that the N^*-TGB_{Ct} transition is always split by the intermediate TGB_{2q} phase. At high b the period of oscillations of $f_{\pm}(x)$ becomes larger than its localization length, and the lowest eigenstate $f_+(x)$ has the single-peak profile of the TGB_A phase. The $N^*-TGB_A-TGB_{Ct}-TGB_{2q}$ tetracritical point M_0 corresponds therefore to the highest in b intersection of t_{\pm} eigentemperatures. As follows from Fig. 3, the appearance of the TGB_{2q} phase becomes practically invisible when b decreases below the second intersection of t_{\pm} at the point M_1 . We expect, therefore, that only the odd TGB_{2q} phase between M_0 and M_1 can be observed in reality.

Equation (11) can be solved analytically in the two limit cases $\sigma_{\parallel} = 0$ and $\sigma_{\parallel} \gg 1$, when the operator $\overline{\mathcal{H}}$ can be truncated to a more simple form. Although the case $\sigma_{\parallel} = 0$ does not correspond to the real situation of $\sigma_{\parallel} > 1$ we consider it first since it clarifies the qualitative structure of the phase diagram that conserves also at large σ_{\parallel} .

B. Case $\sigma_{\parallel} = 0$

When $\sigma_{\parallel} = 0$, operator $\overline{\mathcal{H}}$ is a polynomial Schrödinger operator for the harmonic oscillator:

$$\overline{\mathcal{H}} = \sigma_{\perp}^2 - 2\sigma_{\perp} \left(-\overline{\partial}_x^2 + b^2 \overline{x}^2 \right) + \left(-\overline{\partial}_x^2 + b^2 \overline{x}^2 \right)^2 \quad (14)$$

Therefore, it has the same set of oscillator eigenfunctions:

$$f_n(\overline{x}) = H_n(\sqrt{b}\overline{x})e^{-\overline{x}^2 b/2} \quad (15)$$

where H_n are the Hermitian polynomials. The corresponding eigentemperatures are given by the equation:

$$t_n = 2\sigma_{\perp} (2n + 1) b - (2n + 1)^2 b^2 \quad (16)$$

The oscillations of $t_{c2}(b) = \max t_n(b)$ (Fig.3a) are related to the quantum number n_{c2} of the lowest eigenstate that changes with b , unlike what occurs in the harmonic oscillator where the $n = 0$ eigenlevel is always the lowest one.

When $b > \sigma_{\perp}/2$, the $n = 0$ eigenlevel does correspond to the upper critical temperature $t_{c2} = 2\sigma_{\perp}b - b^2$. The block profile function has a Gaussian shape $e^{-\bar{x}^2 b/2}$ in the TGB_A phase. The slab width is calculated as in [1]:

$$\bar{l}_b = 2.2\varepsilon^{1/2}/b^{1/2} \quad (17)$$

When $b < \sigma_{\perp}/2$, n_{c2} is given by $\sigma_{\perp}/2b - 1/2$ rounded to the nearest integer. The oscillating upper critical temperature $t_{c2}(b)$ tends to σ_{\perp}^2 when b vanishes as shown in Fig. 3a. The slab width is given by the width of the polynomial $H_{n_{c2}}(\sqrt{b}\bar{x})$ as:

$$\bar{l}_b = \sigma_{\perp}^{1/2}/b \quad (18)$$

The block profile function $f_{n_{c2}}(\bar{x})$ oscillates as $\cos(\lambda\bar{x} + \pi n_{c2})$ with period $\lambda = 2\pi/(2n_{c2}b)^{1/2} \simeq 2\pi/\sigma_{\perp}^{1/2}$. This corresponds to the slab of the TGB_{2q} phase which is the superposition of two SmC slabs with layers inclined at $\theta_0 = \pm\sigma_{\perp}^{1/2}$. The parity of $f_n(\bar{x})$ alternates with n resulting in the different parity of $f_{n_{c2}}$ and $f_{n_{c2}\pm 1}$ eigenstates. So, the admixture of $if_{n_{c2}\pm 1}$ eigenfunctions with the TGB_{2q} profile function $f_{n_{c2}}$ that occurs at some critical temperature below t_{c2} corresponds to the TGB_{2q} - TGB_{Ct} transition.

The tetracritical point M_0 , where N^* - TGB_A - TGB_{Ct} - TGB_{Ct} phases meet is given by $b_0 = \sigma_{\perp}/2$, $t_0 = 3\sigma_{\perp}^2/4$

C. Case $\sigma_{\parallel} \gg 1$

In the limit $\sigma_{\parallel} \gg 1$ one can neglect $b^2\bar{x}^2$ in (11) and rewrite $\bar{\mathcal{H}}$ as:

$$\bar{\mathcal{H}} = \left(\bar{\partial}_x^2 + \sigma_{\perp}\right)^2 + \sigma_{\parallel}b^4\bar{x}^4 \quad (19)$$

The eigentemperatures and eigenfunctions of Eq.(19) have in addition to (12) the scaling properties:

$$\begin{aligned} t_n(b, \sigma_{\parallel}, \sigma_{\perp}) &= \sigma_{\perp}^2 \cdot t_{c2}(b\sigma_{\parallel}^{1/4}/\sigma_{\perp}, 1, 1), \\ f_n(\bar{x}, b, \sigma_{\parallel}, \sigma_{\perp}) &= f_n(\sigma_{\perp}^{1/2}\bar{x}, b\sigma_{\parallel}^{1/4}/\sigma_{\perp}, 1, 1). \end{aligned} \quad (20)$$

So, $t_{c2}(b, \sigma_{\parallel}, \sigma_{\perp})$ at large σ_{\parallel} is defined by the universal function $t_{c2}(b, 1, 1)$. We therefore use the scaled coordinates $b\sigma_{\parallel}^{1/4}/\sigma_{\perp}$, t/σ_{\perp}^2 for large σ_{\parallel} to trace $t_{c2}(b)$ that is obtained from numerical diagonalization of (19) (Fig. 3c).

An important conclusion that follows from Fig. 3c is that the phase diagram for large σ_{\parallel} possesses the same features as for $\sigma_{\parallel} = 0$. It includes the domains of the TGB_A and TGB_{2q} phases that precede the transition to the TGB_{Ct} phase. The TGB_A phase exists above the tetracritical point M_0 and the TGB_{2q} phase is important in between the points M_0 and M_1 . From Fig. 3c one locates the points M_0 , M_1 at $b\sigma_{\parallel}^{1/4}/\sigma_{\perp} \simeq 0.36$ and $b\sigma_{\parallel}^{1/4}/\sigma_{\perp} \simeq 0.19$.

Consider now the transition to the TGB_C phase at low field $b \ll 0.36\sigma_{\perp}/\sigma_{\parallel}^{1/4}$ (i.e., below M_0) and to the TGB_A phase at high field $b \gg 0.36\sigma_{\perp}/\sigma_{\parallel}^{1/4}$ (i.e., above M_0). Both the asymptotics for $t_{c2}(b)$ are shown in Fig. 3c by the dashed lines.

Low fields: $b \ll 0.36\sigma_{\perp}/\sigma_{\parallel}^{1/4}$

At low field when the block width \bar{l}_b diverges, one can assume that blocks have the structure of *SmC* slabs where the inclination of layers to the pitch axis is equal to its bulk value $\theta_0 = \pm \arctan \sigma_{\perp}^{1/2}$. Then the block's profile function $f(\bar{x})$ has a high-frequency modulation $e^{\pm i\sigma_{\perp}^{1/2}\bar{x}}$ where + and - signs correspond to right and left tilting respectively. This factor can be excluded by shift: $\bar{\partial}_x \rightarrow \bar{\partial}_x \pm i\sigma_{\perp}^{1/2}$ in Eq.(19). Next, we neglect $\bar{\partial}_x^2$ in comparison with $2\sigma_{\perp}^{1/2}\bar{\partial}_x$ (justification of this approximation will be given below) and write $\bar{\mathcal{H}}$ as:

$$\bar{\mathcal{H}} = -\left(2\sigma_{\perp}^{1/2}\bar{\partial}_x\right)^2 + \sigma_{\parallel}b^4\bar{x}^4 \quad (21)$$

Rescaling \bar{x} as: $\zeta = (b^4\sigma_{\parallel}/4\sigma_{\perp})^{1/6}\bar{x}$ simplifies (21) to an unharmonic oscillator operator:

$$\bar{\mathcal{H}} = \left(16\sigma_{\perp}^2\sigma_{\parallel}\right)^{1/3} b^{4/3} \left(-\partial_{\zeta}^2 + \zeta^4\right) \quad (22)$$

Finally, $t_{c2}(b)$ and the corresponding eigenfunction of (21) are given by:

$$\begin{aligned} t_{c2} &= \sigma_{\perp}^2 - 1.06 \cdot \left(16\sigma_{\perp}^2\sigma_{\parallel}\right)^{1/3} b^{4/3} \\ f_{c2}(\bar{x}) &= e^{\pm i\sigma_{\perp}^{1/2}\bar{x}} \cdot g_1 \left(\left(b^4\sigma_{\parallel}/4\sigma_{\perp}\right)^{1/6}\bar{x}\right) \end{aligned} \quad (23)$$

where 1.06 and $g_1(\zeta)$ are the lowest eigenvalue and eigenfunction of the unharmonic oscillator equation: $(-\partial_{\zeta}^2 + \zeta^4)g_1 = 1.06g_1$. The block width \bar{l}_b is estimated as the characteristic width $\sim (4\sigma_{\perp}/b^4\sigma_{\parallel})^{1/6}$ of the function g_1 . More accurately, we can calculate \bar{l}_b in the same way as was done in [1] for the *TGB_A* phase, using the suitable Gaussian approximation for $g_1(\zeta)$ as $e^{-0.4\zeta^2}$. Finally we get:

$$\bar{l}_b = 3.2\varepsilon^{1/2}(\sigma_{\perp}/b^4\sigma_{\parallel})^{1/6} \quad (24)$$

At first glance, the eigenstate (23) is doubly degenerate with respect to a sign change in the modulation phase $e^{\pm i\sigma_{\perp}^{1/2}\bar{x}}$. However, this is an artifact of the approximation: the term $\bar{\partial}_x^2$ we are neglecting lifts the degeneracy and splits the transition onto two. In particular, in between the points M_0 and M_1 (Fig3c) $\bar{\partial}_x^2$ favors the odd *TGB_{2q}* phase given by the linear combination $(e^{i\sigma_{\perp}^{1/2}\bar{x}} - e^{-i\sigma_{\perp}^{1/2}\bar{x}}) \cdot g_1 = 2ig_1 \sin \sigma_{\perp}^{1/2}\bar{x}$. The *TGB_{Ct}* profile appears by means of an additional transition when the even combination $\sim 2ig_1 \cos \sigma_{\perp}^{1/2}\bar{x}$ admixes.

This effect, however, is as tiny (and negligible below M_1) as $\langle \bar{\partial}_x^2 \rangle \simeq 1/\bar{l}_b^2$ is smaller than $\langle 2\sigma_{\perp}^{1/2}\bar{\partial}_x \rangle \simeq 2\sigma_{\perp}^{1/2}/\bar{l}_b$, where \bar{l}_b is given by Eq.(24) and $b \ll 0.36\sigma_{\perp}/\sigma_{\parallel}^{1/4}$. The above estimation confirms the selfconsistency of the approximation we made. Condition $b \ll 0.36\sigma_{\perp}/\sigma_{\parallel}^{1/4}$ is equivalent to the requirement that the wavelength of the transversal modulation $\lambda \sim \sigma_{\perp}^{-1/2}$ is smaller than the block width \bar{l}_b given by (24). This clarifies the physical meaning of the approximation.

High fields: $b \gg 0.36\sigma_{\perp}/\sigma_{\parallel}^{1/4}$

Neglecting now σ_{\perp} in comparison with $\bar{\partial}_x^2$ we simplify $\bar{\mathcal{H}}$ as:

$$\overline{\mathcal{H}} \simeq \overline{\partial}_x^4 + \sigma_{\parallel} b^4 \overline{x}^4 \quad (25)$$

Then t_{c2} and the corresponding eigenfunction are given by:

$$t_{c2} \simeq -1.39 \cdot \sigma_{\parallel}^{1/2} b^2 \quad f_{c2}(\overline{x}) = g_2\left(\sigma_{\parallel}^{1/8} b^{1/2} \overline{x}\right) \quad (26)$$

where 1.39 and $g_2(\eta)$ are the lowest eigenvalue and eigenfunction of the operator $\partial_{\eta}^4 + \eta^4$. Unlike the low field case, the eigenstate (25) is nondegenerate and described by the even bell-shaped function g_2 , the lowest odd eigenstate being well separated from g_2 as shown in Fig. 3c.

The eigenfunction $g_2\left(\sigma_{\parallel}^{1/8} b^{1/2} \overline{x}\right)$ gives the TGB_A - like profile of the block. The block width \overline{l}_b is calculated using the results of [1] by noting that $g_2(\eta) \sim e^{-0.55\eta^2}$:

$$\overline{l}_b = 2.1\varepsilon^{1/2}/\sigma_{\parallel}^{1/8} b^{1/2} \quad (27)$$

The approximation we made is self-consistent since $\langle \overline{\partial}_x^2 \rangle \simeq 1/\overline{l}_b^2$ is indeed greater than σ_{\perp} when $b \gg 0.36\sigma_{\perp}/\sigma_{\parallel}^{1/4}$. Considering the truncated term $\hat{h} = 2\sigma_{\perp}\overline{\partial}_x^2 + \sigma_{\perp}^2$ as a perturbation, one improves the asymptotic for $t_{c2}(b)$. The correction to t_{c2} is given by $\langle g_2 | \hat{h} | g_2 \rangle \simeq 2\gamma\sigma_{\parallel}^{1/4}\sigma_{\perp}b + \sigma_{\perp}^2$ where $\gamma = \langle g_2 | \partial_{\eta}^2 | g_2 \rangle \simeq 0.5$. Finally, we get:

$$\begin{aligned} t_{c2} &\simeq \sigma_{\parallel}^{1/4} \sigma_{\perp} b - 1.39\sigma_{\parallel}^{1/2} b^2 \\ &= -1.39 \cdot (\sigma_{\parallel}^{1/4} b - 0.36\sigma_{\perp})^2 + 0.18\sigma_{\perp}^2 \end{aligned} \quad (28)$$

In fact, the asymptotic (28) is valid also in the region of small negative σ_{\perp}/b . It makes the analogous expressions in [14,15] more precise and explicitly determines all the coefficients.

D. Stability of the TGB_{Ct} state.

Having calculated the transition temperature and structure of the TGB_{Ct} phase we discuss now its stability, namely, whether this phase has the highest upper critical temperature t_{c2} (or, alternatively, the highest upper critical field, b_{c2}) among other TGB states and under which condition a transition from N^* to SmC^* occurs via the intermediate TGB_{Ct} phase rather than via the direct first order transition.

To answer the first question, consider the competing TGB_{Ct} and TGB_{Cp} phases that can be formed at the N^* - SmC^* transition. Dozov's estimation of the ratio of their upper critical fields [17], gives the factor $2\left(C_{\parallel}/2Dq_0^2\right)^{1/4} = 2(2\sigma_{\parallel})^{1/4}$ which is larger than one as long as $\sigma_{\parallel} > 1$. Therefore, $b_{c2}(TGB_{Ct}) > b_{c2}(TGB_{Cp})$ and the TGB_{Ct} phase is indeed more preferable.

Our calculations are in agreement with Dozov's estimation. To show this, compare $t_{c2}(TGB_{Ct})$ given by Eq.(23) with $t_{c2}(TGB_{Cp})$ calculated in [15]:

$$t_{c2}(TGB_{Cp}) \simeq \sigma_{\perp}^2 - 1.06 \cdot (1 + \sigma_{\parallel})^{1/3} \left(16\sigma_{\perp}^2\sigma_{\parallel}\right)^{1/3} b^{4/3} \quad (29)$$

(We recalculated the numerical factor 1.06). The ratio of the upper critical fields for the TGB_{Ct} and TGB_{Cp} phases (at given temperature) is expressed as $(1 + \sigma_{\parallel})^{1/4}$, which is larger than one. This is consistent with Dozov's estimation when $\sigma_{\parallel} \gg 1$, but gives a more precise value of the numerical factor. Although the starting GL functional (4) is slightly different from that, used in [15] (see our remark after Eq.(4)), this does not change the final result: one can show that in a relevant limit, $\sigma_{\parallel} \gg \sigma_{\perp}$, expressions for $b_{c2}(TGB_{Ct})$ calculated for both the functionals are the same. Note that standard perturbational analysis proves that the TGB_{Ct} and TGB_A phases are stable with respect to small parallel tilting of the layers when angle φ in Eq.(9) becomes nonzero.

To answer the second question, note that transition via an intermediate TGB state is not preempted by the direct N^* - Sm transition when the upper critical temperature t_{c2} for the TGB state is larger than the thermodynamical temperature t_c of the direct transition. Recall first the calculations for the TGB_A phase when $\sigma_{\perp} < 0$ [1]. Comparison of t_{c2} given by Eq.(13) (without $(1 + 3\sigma_{\parallel}/4)b^2$) with the N^* - SmA transition temperature T_{N^*A} (6), which in dimensionless units is written as:

$$t_c = (gK_2)^{1/2}b/Dq_0^3 \quad (30)$$

gives the following criterion for stability of the TGB_A phase:

$$\kappa_2 > 1/\sqrt{2} \quad \text{where} \quad \kappa_2 = (gK_2/2\sigma_{\perp}^2)^{1/2}/2Dq_0^3 \quad (31)$$

When $\sigma_{\perp} > 0$ the t_{c2} transition temperature for TGB_{Ct} is given by Eq.(23), and the N^* - SmC^* transition temperature $T_{N^*C^*}$ (6) in dimensionless units is written as:

$$t_c \simeq \sigma_{\perp}^2 - \frac{(gK_2)^{1/2}}{Dq_0^3}(1 - \sigma_{\perp}K_2/2K_3)b \quad (32)$$

The criterion $t_{c2} > t_c$ is always satisfied when b is small enough, since at small b , t_c is linear in b and t_{c2} is proportional to $b^{4/3}$. So, strictly speaking, one can always obtain the TGB_{Ct} phase by preparation of the nearly racemic binary mixture of the left and right chiral molecules. The above consideration is valid only if $t_c(b)$ has a positive slope, that is, when $\sigma_{\perp} < 2K_3/K_2$. This condition was used in [15,16] as a criterion for stability of the TGB_C state. It is not very likely, however, to find a system where this condition will not be the case since in conventional SmC^* liquid crystals $\sigma_{\perp} < 1$ and $2K_3/K_2 \simeq 4-6$ [19]. In contrast, the practical identification of this small- b TGB_{Ct} phase can be quite difficult because of the very large cholesteric pitch. We formulate the realistic criterion for the existence of the TGB_{Ct} phase as a condition when it is stable in the vicinity of the critical point M_0 . On the basis of the plot in Fig. 3c, one obtains that $t_{c2} > t_c$ near M_0 if:

$$\kappa_2 > 0.5\sigma_{\parallel}^{1/4}. \quad (33)$$

At realistic values of $\sigma_{\parallel} \simeq 10-100$ [24] this condition practically coincides with criterion for stability of the TGB_A phase (31). The conditions (31) and (33) determine the position of the critical points M_A and M_C on the N^* - SmA, C^* transition line of Fig.1 where the TGB_A and TGB_C phases first appear.

E. Resume

We have revised the calculations of [15] for the N^* - $TGB_{A,Ct}$ phase transition. The line of the upper critical temperature on phase diagram of Fig.1 is reconstructed on the quantitative level and can be present in the relevant limit $\sigma_{\parallel} > 1$ as follows:

On the left side of the point M_A that is defined by condition (31), the direct N^* - SmA first order transition takes place. The critical temperature of the transition is given by (30).

Between the points M_A and M_0 the transition to the TGB_A phase occurs. The point M_0 is placed at $0.36\sigma_{\perp} \simeq \sigma_{\parallel}^{1/4}b$, inside the region $\sigma_{\perp} > 0$. The upper critical temperature t_{c2} of the transition is given by (13) when $-\sigma_{\perp}/b > 0.5 + 0.38\sigma_{\parallel}$, and by (28) when σ_{\perp}/b varies from a small negative value to $\sigma_{\perp}/b \simeq \sigma_{\parallel}^{1/4}/0.36$. Both the asymptotics are matched in the intermediate region of negative σ_{\perp}/b .

In between the points M_0 and M_C the sequence of transitions N^* - TGB_{2q} - TGB_{Ct} takes place, the location of the point M_C being given by the condition (33). The TGB_{2q} phase exists in a small temperature interval below t_{c2} . It practically disappears on the right of the point M_1 where $\sigma_{\perp}/b > \sigma_{\parallel}^{1/4}/0.19$. The upper critical temperature in between M_0 and M_C is given by Eq.(23). The junction of t_{c2} transition lines for TGB_A and TGB_{2q}/TGB_{Ct} phases forms a kink in the tetracritical point M_0 .

On the right side of the point M_C the direct first order N^* - SmC^* transition occurs at the critical temperature t_c , as is given by Eq.(32)

We have also calculated the width \bar{l}_b of the TGB slab at $T = T_{c2}$ with respect to different parameters $b, \sigma_{\perp}, \sigma_{\parallel}$ (Eqns. (17), (18), (24) and (27)). We summarize these results in Table I by the ratio $l_b/l_d = \bar{l}_b/\bar{l}_d = \bar{l}_b^2 b/2\pi$, resulting from the topological constraint (1).

IV. ANALOGY WITH SPACE-MODULATED SUPERCONDUCTIVITY

In this section we discuss a remarkable similarity between the TGB state and the mixed (vortex state) in superconductors of type II noted first in [1]. We show that the TGB_C phase corresponds to the mixed state in the "exotic" superconductors with space modulated order parameter.

Note first that, due to de Gennes [18,19] the $N - SmA$ transition is analogous to the superconducting phase transition because of similarity of the transformational properties of the order parameters: the space modulated function $\psi(r) = \psi_0 e^{q_0 \mathbf{n} \cdot \mathbf{r}}$ in SmA and the complex wave function $\Psi(r)$ in superconductor. The translation of $\psi(r)$ along the modulation vector $q_0 \mathbf{n}$ (that is equivalent to multiplication of ψ on a phase factor) corresponds to the gauge transformation in the superconductor.

The long range twist of $\mathbf{n}(r)$ in N^* plays the role of the magnetic field destroying superconductivity. The N^* - SmA transition via the intermediate TGB_A phase occurs with continuous Meissner-like expulsion of the twist of \mathbf{n} . The rows of the screw dislocations resemble the Abrikosov vortex lattice.

The SmC phase is characterized by the additional, transversal to \mathbf{n} modulation of the order parameter resulted from the negative gradient terms in the CL model. Continuing the analogy with superconductivity one can tell that N - SmC transition corresponds to the transition to the superconducting state with nonuniform, space modulated order parameter.

The TGB_C phase therefore should be an analog of the mixed (Abrikosov) state of modulated superconductor, providing that magnetic field is perpendicular to the modulation.

On the quantitative level, the modulated superconductor in a magnetic field is described by the GL equation:

$$t\psi + g|\Psi|^2\Psi = C_{\perp}(i\nabla - \mathbf{A})^2\psi + D(i\nabla - \mathbf{A})^4\psi \quad (34)$$

where \mathbf{A} is the vector potential of the field: $\mathbf{B} = \text{curl}\mathbf{A}$. The modulation of the superconducting order parameter is provided by the gradient term with $C_{\perp} < 0$. The upper critical field of this superconductor is calculated by neglecting the nonlinear term $g|\Psi|^2\Psi$ and solving the corresponding eigenproblem. It is easy to show that if \mathbf{A} is chosen in the Landau gauge $(0, Bx, 0)$, this procedure is exactly reduces to the case " $\sigma_{\parallel} = 0$ " we considered in Sect. IIIB. According to calculations of Sect. IIIB, this superconductor should have the oscillating upper critical field, shown in Fig. 3a.

It is interesting to note that although the theory of space modulated superconductor was considered by Larkin and Ovchinnikov [20] and Fulde and Ferrel [21] more than thirty years ago, to our knowledge no direct experimental observation of this phase currently exists.

Note finally another interesting analogy between the N^* - $TGB_{A,Ct}$ phase transition and the B_{c2} transition in "unconventional" multicomponent superconductor UPt_3 where the kink-like behavior of B_{c2} was observed [22]. The kink point in B_{c2} in UPt_3 is similar to the point M_0 in the N^* - $TGB_{A,Ct}$ phase diagram: both points are provided by the intersection of eigenstates of the corresponding linearized GL equations.

ACKNOWLEDGMENTS

I am grateful to Monique Brunet who drew my attention to the problem and to Laurence Navailles and Philip Barois for fruitful discussions of the experimental aspects. This work was supported by the Brazilian Agency Fundacao de Amparo a Pesquisa em Minas Gerais (FAPEMIG) and by Russian Foundation of Fundamental Investigations (RFFI), Grant No. 960218431a. Part of the work was done during my stay in Université Montpellier II, France.

REFERENCES

* E-mail: lukyanc@itp.ac.ru

- [1] S. R. Renn and T. C. Lubensky, Phys. Rev. **A38**, 2132 (1988).
- [2] J. W. Goodby, M. A. Waugh, S. M. Stein *et al.*, Nature (London) **337**, 449 (1989).
- [3] J. W. Goodby, M. A. Waugh, S. M. Stein *et al.*, J. Am. Chem. Soc. **111**, 8119 (1989).
- [4] G. Srajer, R. Pindak, M. A. Waugh, *et al.*, Phys. Rev. Lett. **64**, 1545 (1990).
- [5] K. J. Ihn, J. A. N. Zasadzinski, R. Pindak, *et al.*, Science **258**, 275 (1992).
- [6] L. Navailles, P. Barois and H. T. Nguyen, Phys.Rev. Lett. **71**, 545 (1993).
- [7] L. Navailles, R. Pindak, P. Barois and H. T. Nguyen, Phys. Rev. Lett., **42**, 5224 (1995).
- [8] L. Navailles, Ph.D. Thesis, L'Universite Bordeaux I (1994).
- [9] H. T. Nguyen, A. Bouchata, L. Navailles, *et al.*, J. Phys. II France **2**, 1889, (1992).
- [10] L. Navailles, H. T. Nguyen, P. Barois, *et al.*, Liq. Cryst., **20**, 653 (1996)..
- [11] L. Navailles, C. W. Garland, J. Phys. II France, **6**, 1243 (1996).
- [12] A. Anakkar, A. Daoudi, J.-M. Buisine, *et al.*, J. Therm. Anal., **41**, 1501 (1994).
- [13] A. Anakkar, A. Daoudi, J.-M. Buisine, *et al.*, Liq. Cryst., **20**, 411 (1996).
- [14] T. C. Lubensky and S. R. Renn, Phys. Rev. **A41**, 4392 (1990).
- [15] S. R. Renn, Phys. Rev. **A45**, 953 (1992).
- [16] S. R. Renn and T. C. Lubensky, Mol. Cryst. Liq. Cryst. **209**, 349 (1991).
- [17] I. Dozov, Phys.Rev. Lett. **74**, 4245 (1995).
- [18] P. G. de Gennes, Solid State Commun. **14**,997 (1972).
- [19] P. G. de Gennes and J. Prost, *The Physics of Liquid Crystals* (Oxford University Press, 1993).
- [20] A. I. Larkin, Y. N. Ovchinnikov, JETP, **47**,1136 (1964).
- [21] P. Fulde and R. A. Ferrel, Phys. Rev. **135**, 555 (1964).
- [22] For a review see: I. Luk'yanchuk, M.Zhitomirsky, Superconductivity review, **1**, 207, (1995).
- [23] Jing-huei Chen and T. C. Lubensky, Phys. Rev. **A14**, 1202 (1976).
- [24] L. J. Martinez-Miranda, A. R. Kortan, and R. J. Birgeneau, Phys. Rev. Lett. **56**, 2264 (1986).

TABLES

TABLE I. Location of the tetracritical point M_0 and the ratio l_b/l_d in a different limit cases. Parameter ϵ varies from 0 when $K_{1,3}/K_2 = 0$ to 1.5 when $K_{1,3}/K_2$ is large.

	Location of M_0		l_b/l_d ^a	
	b_0	t_0	$TGB_A,$ $b > b_0$	$TGB_{2q,Ct},$ $b < b_0$
$\sigma_{\parallel} \ll 1$	$0.5\sigma_{\perp}$	$0.75\sigma_{\perp}^2$	0.8ϵ	$\sigma_{\perp}/2\pi b$
$\sigma_{\parallel} \gg 1$	$0.36\sigma_{\perp}/\sigma_{\parallel}^{1/4}$	$0.43\sigma_{\perp}^2$	$0.7\epsilon\sigma_{\parallel}^{-1/4}$	$\epsilon(4\sigma_{\perp}/b\sigma_{\parallel})^{1/3}$

^aThe ratio l_b/l_d is given at N^* - TGB transition line. At lower temperatures l_b/l_d increases rapidly.

FIGURES

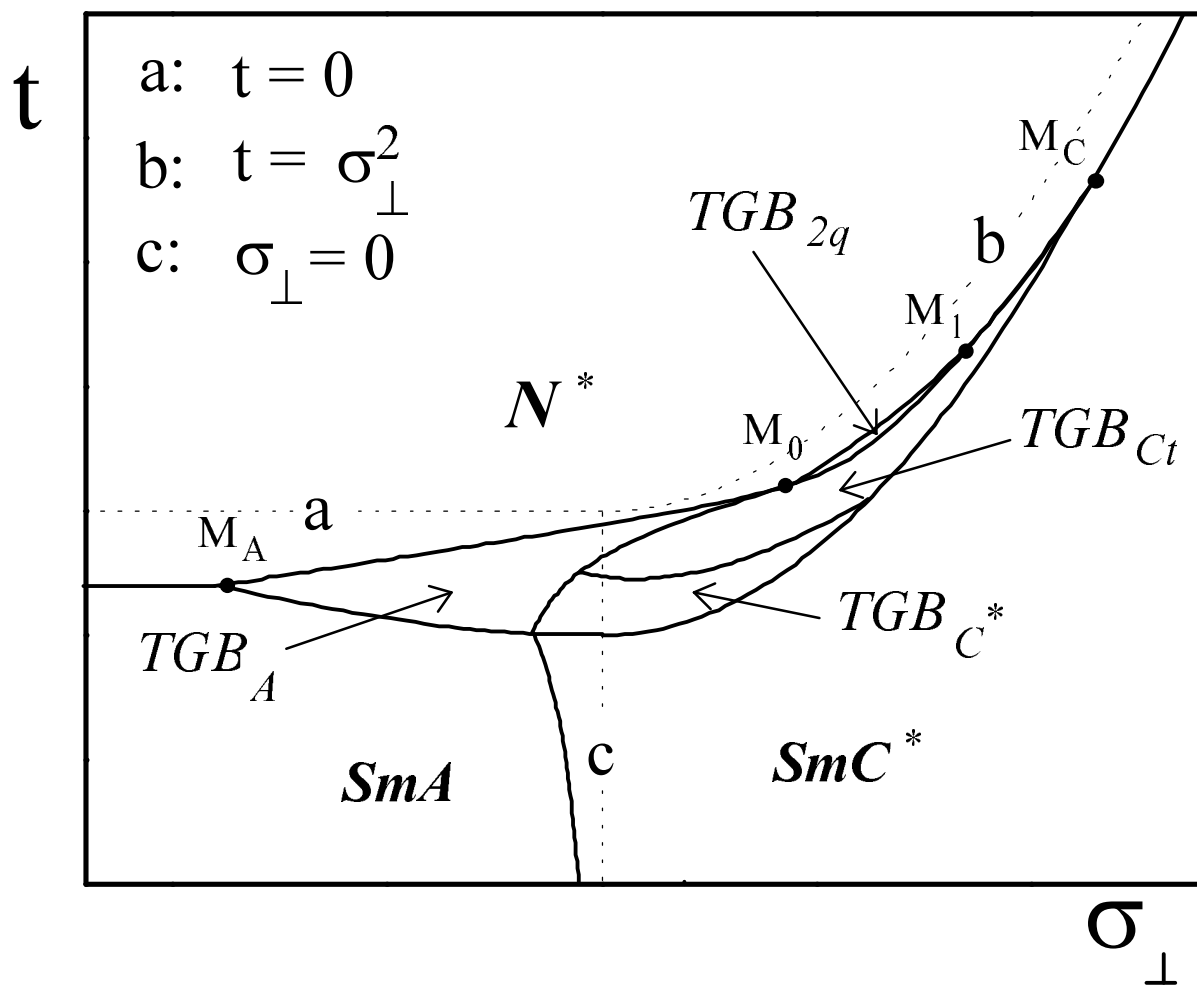


FIG. 1. The phase diagram of TGB phases. The model parameters t, σ_{\perp} are controlled by the experimental conditions. We predict a new TGB_{2q} phase and penetration of the TGB_A phase in the SmC^* region where $\sigma_{\perp} > 0$. Dotted lines a, b and c present the $N - SmA - SmC$ diagram in the nonchiral case.

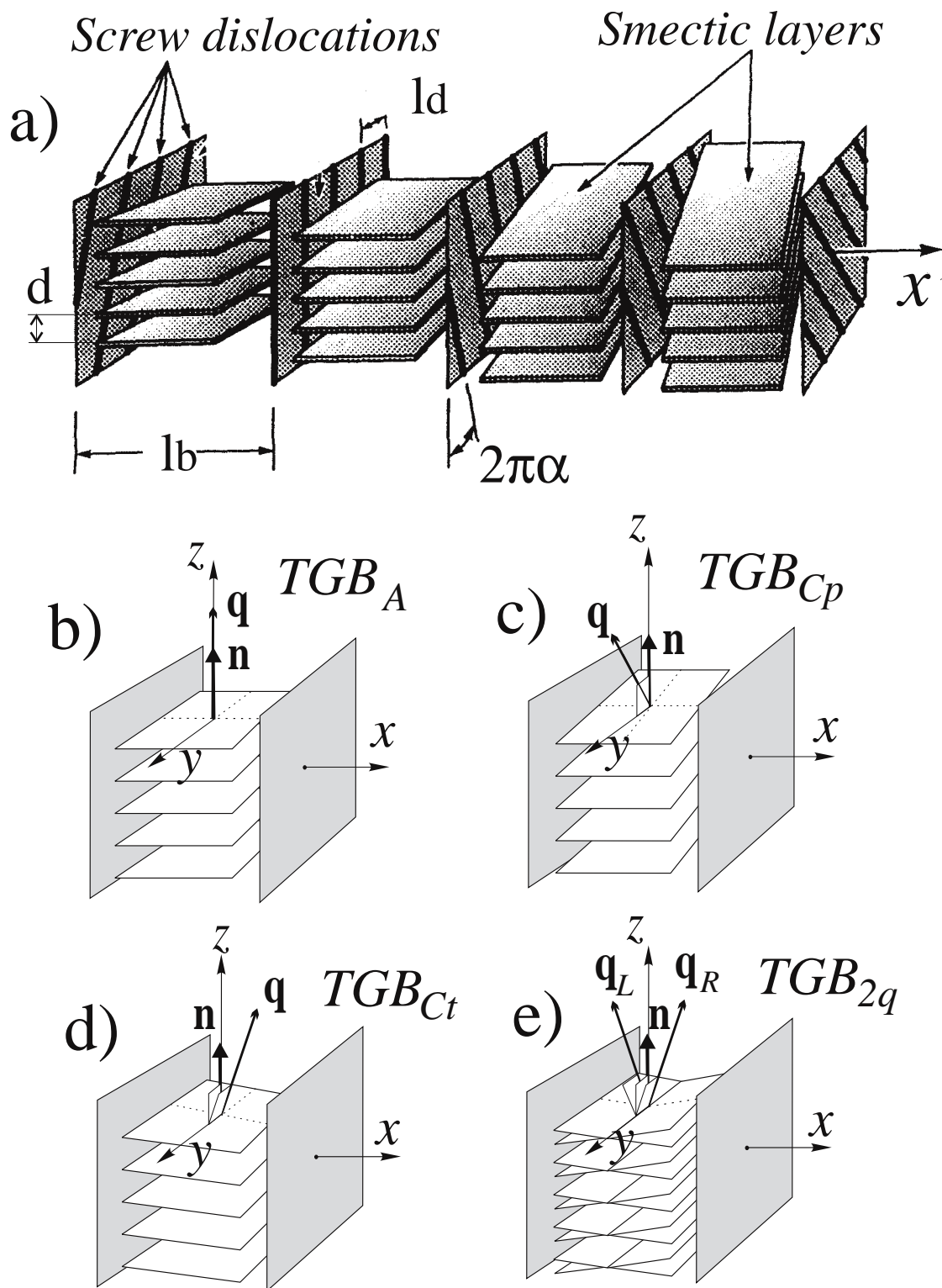


FIG. 2. Structure of different TGB phases.

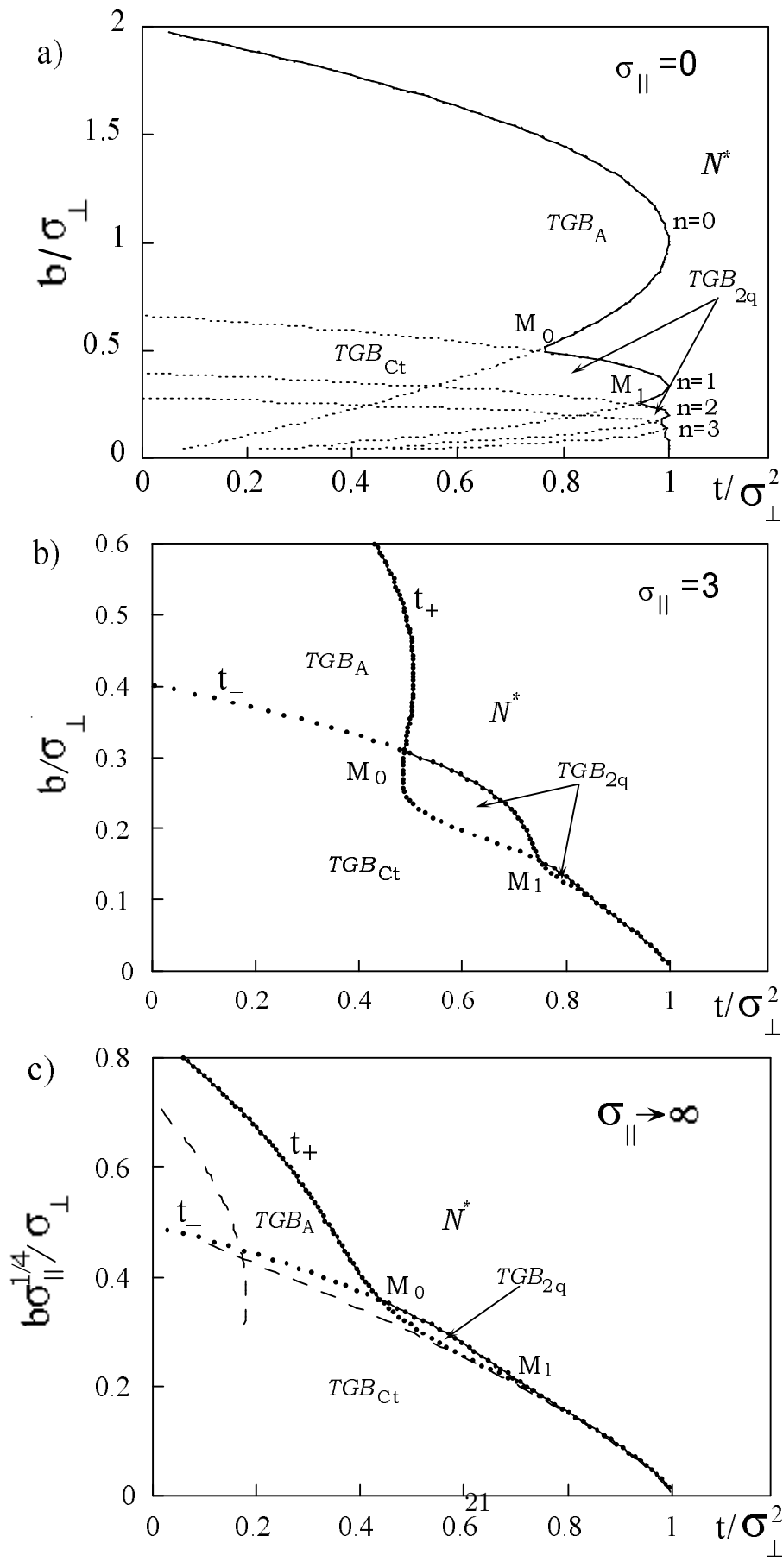


FIG. 3. Oscillating behavior of the lowest eigenstates of the linearized CL model that correspond the Cholesteric (N^*) - TGB_{Ct} transition as a function of the model parameters: t/σ_{\perp}^2 , b/σ_{\perp} and σ_{\parallel} . The concurrence between two nearly degenerate lowest eigenlevels (the minimal one corresponds to t_{c2}) leads to splitting of the transition by appearance of either the TGB_A phase or the intermediate TGB_{2q} phase. Dashed lines in (c) present the asymptotics calculated in the text.